THE JOURNAL OF BIOLOGICAL CHEMISTRY
Vol. 277, No. 44, Issue of November 1, pp. 41916–41924, 2002
Printed in U.S.A.

Two-step Membrane Binding by Equinatoxin II, a Pore-forming Toxin from the Sea Anemone, Involves an Exposed Aromatic Cluster and a Flexible Helix*

Received for publication, May 13, 2002, and in revised form, August 26, 2002
Published, JBC Papers in Press, August 26, 2002, DOI 10.1074/jbc.M204625200

Qi Hong‡§, Ion Gutiérrez-Aguirre§¶, Ariana Barlič¶, Petra Malovrh‖, Katarina Kristan‖, Zdravko Podlesek‖, Peter Maček‖, Dušan Turk, Juan M. González-Mañas¶, Jeremy H. Lakey‡, and Gregor Anderluh‡‖‡‡**

*From the ‡School of Biochemistry and Genetics, University of Newcastle upon Tyne, Framlington Place, Newcastle upon Tyne, NE2 4HH, United Kingdom, the ¶Unidad de Biofisica (CSIC-UPV/EHU) and Departamento de Bioquimica y Biologia Molecular, Universidad del Pais Vasco, Apartado 644, 48080 Bilbao, Spain, the ‖Department of Biology, Biotechnical Faculty, University of Ljubljana, Večna pot 111, 1000 Ljubljana, Slovenia, and the **Department of Biochemistry and Molecular Biology, Jožef Stefan Institute, Jamova 39, 1000 Ljubljana, Slovenia*

Equinatoxin II (EqtII) belongs to a unique family of 20-kDa pore-forming toxins from sea anemones. These toxins preferentially bind to membranes containing sphingomyelin and create cation-selective pores by oligomerization of 3–4 monomers. In this work we have studied the binding of EqtII to lipid membranes by the use of lipid monolayers and surface plasmon resonance (SPR). The binding is a two-step process, separately mediated by two regions of the molecule. An exposed aromatic cluster involving tryptophans 112 and 116 mediates the initial attachment that is prerequisite for the next step. Steric shielding of the aromatic cluster or mutation of Trp-112 and -116 to phenylalanine significantly reduces the toxin-lipid interaction. The second step is promoted by the N-terminal amphiphilic helix, which translocates into the lipid phase. The two steps were distinguished by the use of a double cysteine mutant having the N-terminal helix fixed to the protein core by a disulfide bond. The kinetics of membrane binding derived from the SPR experiments could be fitted to a two-stage binding model. Finally, by using membrane-embedded quenchers, we showed that EqtII does not insert deeply in the membrane. The first step of the EqtII binding is reminiscent of the binding of the evolutionarily distant cholesterol-dependant cytolysins, which share a similar structural motif in the membrane attachment domain.

Targeting and attachment of proteins to membranes is one of the key steps in many cellular processes (1–3). Protein-membrane interactions have been studied intensively in recent years with many different examples of proteins and membranes. These interactions can be promoted at the lipid-water interface by lipid anchors, electrostatic forces or surface-exposed aromatic and aliphatic residues (1, 2, 4). Compared with protein-protein interactions, details of protein-membrane interactions are poorly defined. Some of the best characterized examples are a phospholipase C pleckstrin homology domain specific for phosphatidylinositol trisphosphate (5) and small protein kinase-C-conserved (C2) domains specific for zwitterionic, particularly phosphatidylcholine membranes (6).

Another group of proteins interacting with lipid membranes are pore-forming toxins (PFT)[1] (7–10), which bind to membranes before eliciting their toxic effects via the formation of transmembrane pores. The most studied PFT are bacterial since this group includes important virulence factors. Few examples of eukaryotic PFT have been well characterized, exceptions being the actinoporins, cytolysins found exclusively in sea anemones (10, 11). Members of this family have properties distinct from other PFT: they are composed of 175–179 amino acids, contain no cysteine residues, have pI>9.5, and show a preference for sphingomyelin (SM)-containing membranes. Actinoporins act on cellular and model lipid membranes by forming cation-selective pores with a hydrodynamic diameter of ~2 nm. The mechanism of pore formation involves at least two steps: binding of the water soluble monomer to the membrane; and subsequent oligomerization of three to four monomers on the surface of the membrane, leading to the formation of a functional pore (10, 12–16). The number of monomers in the final pore was deduced from cross-linking (12) and kinetic experiments (16). The N-terminal amphiphilic α-helix, which is well conserved in actinoporins, has been proposed to participate in formation of the transmembrane channel (17–19). This suggestion was recently supported by crystal and NMR structures of equinatoxin II, an actinoporin isolated from the sea anemone *Actinia equina* (EqtII) (20, 21). The EqtII molecule is composed of a hydrophobic β-sandwich core, flanked on each side by α-helices. The first 30 N-terminal residues, including the amphiphilic helix, form the largest segment of the molecule able to adopt a different structure without disrupting the general fold of the molecule. Another interesting feature of the

* This work was supported in part by a grant from the Slovenian Ministry of Education, Science and Sport, the BBSRC, and the Wellcome Trust (Equipment Grants 56232, 40422, 55979) (to Q. H. and J. H. L.), a long-term FEBS fellowship (to G. A.), a postdoctoral fellowship from the Basque government (to A. B.), and Grant PI-1998-110 from the Basque Government (to I. G. A. and J. M. G.-M.). The costs of publication of this article were defrayed in part by the payment of page charges. This article must therefore be hereby marked "*advertisement*" in accordance with 18 U.S.C. Section 1734 solely to indicate this fact.

§ These authors contributed equally to the work.

‡‡ To whom correspondence should be addressed. Tel.: 386-1-423-33-88; Fax: 386-1-257-33-90; E-mail: gregor.anderluh@ncl.ac.uk or gregor.anderluh@uni-lj.si.

[1] The abbreviations used are: PFT, pore-forming toxins; ANTX, aminonaphtalene-1,3,6,-trisulfonic acid; CDC, cholesterol-dependent cytolysins; DOPC, 1,2-dioleoyl-*sn*-glycero-3-phosphocholine; DP-mercapto-PA, *O*-(8′-mercapto-3′,6′-dioxaoctyl)-1,2-dipalmitoyl-*sn*-glycero-3-phosphatidic acid; DPPC, dipalmitoylphosphatidylcholine; EqtII, equinatoxin II; DPX, *p*-xylene-bis-pyridiniumbromide; LUV, large unilamellar vesicles; L/T, lipid/toxin; PC, phosphatidylcholine; PLA_2, phospholipase A_2; SM, sphingomyelin; SPR, surface plasmon resonance; SUV, small unilamellar vesicles.

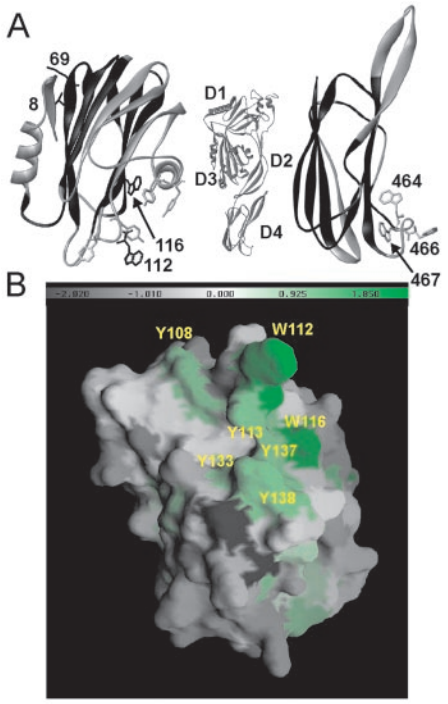

FIG. 1. **Three-dimensional structure of EqtII and structurally similar fourth domain of perfringolysin.** *A*, models of EqtII (*left*) and fourth domain of perfringolysin (PFO) (*right*) are shown. The model of the whole PFO molecule is shown in the middle with designated domains 1–4. The regions, which were identified as structurally similar by DALI (53), are denoted *black*. Side chains of aromatic amino acids from the conserved aromatic clusters of EqtII and PFO are shown. The amino acids of EqtII, which were mutated in this study, are shown in *black* and are designated with numbers. *B*, the surface of EqtII aromatic patch. Amino acids are colored according to the experimentally determined scale for partitioning into the lipid-water interface (White-Wimley scale) (24). The picture was generated with GRASP (54).

structure is a cluster of exposed aromatic amino acid residues on the surface of the molecule, comprising Tyr-108, Trp-112, Tyr-113, Trp-116, Tyr-133, Tyr-137, and Tyr-138 (Fig. 1*B*). These are likely to have a role in membrane recognition and binding since aromatic residues have been shown to have affinity for the lipid-water interface (22–24). These observations led to our current hypothesis for EqtII pore formation, which proposes that the toxin initially binds the membrane via the aromatic cluster. In the next step the N-terminal helix translocates from the surface of the β-sandwich to the membrane and, finally, traverses the lipid bilayer forming the cation-selective pore.

The actinoporins have no obvious sequence similarity to any other proteins. Structural similarity (with very low sequence similarity) was observed with thaumatin and the fourth (C-terminal) domain of perfringolysin O (PFO) (20). These proteins are rich in β-sheet, and their similarity to EqtII is confined within the β-sandwich region (Fig. 1*A*). PFO is a representative of the cholesterol-dependent cytolysin (CDC) group of toxins (25). It is a 500-residue protein composed of four domains (Fig. 1*A*) (26). It can form huge pores with a diameter of up to 150 nm, made up of more than 30 monomers. PFO attaches to membranes via domain 4, which contains an undecapeptide sequence (^{458}ECTGLAWEWWR^{468}) extremely conserved among different members of CDC (25, 27) and similar to the EqtII tryptophan-rich region (^{110}YNWYSNWW^{117}). Tryptophans within the undecapeptide motif were shown to have a role in membrane attachment (28). Furthermore, these tryptophans are not transferred deeply into the lipid bilayer according to fluorescence results using membrane embedded quenchers (27). Although the final steps of pore-formation are different in the two groups of toxins (10, 25), the initial membrane interaction might be similar due to similarities both in the structure of the membrane binding domain and the presence of exposed tryptophans.

In this work we report the results of studies on the molecular details of the binding of EqtII to model membranes using a range of mutants and biophysical approaches. We show that the most important region for the membrane binding is the aromatic cluster. The mutation of exposed Trp-112 and Trp-116 to phenylalanine significantly reduced binding as viewed by monolayer and SPR experiments. Furthermore, by creating an engineered disulfide bridge, which prevented dislocation of the helix from the body of the molecule, we were able to distinguish between the two binding steps: initial binding to the membranes and insertion into the membrane of the N-terminal helix. The latter provides additional contacts with the membrane and leads to a largely irreversible insertion. According to the fluorescence results, EqtII does not insert deeply in the bilayer. The initial binding step of EqtII is reminiscent of the CDC toxins, thus there exists not only structural, but also functional similarity between the two groups of otherwise unrelated toxins.

EXPERIMENTAL PROCEDURES

Materials—Brain Sphingomyelin (SM) and dipalmitoylphosphatidylcholine (DPPC) were from Avanti Polar Lipids (Alabaster, AL). Egg phosphatidylcholine (PC) was from Lipid Products (South Nutfield, UK). Brominated lipids 1-palmitoyl-2-stearoyl-(6,7)-dibromo-*sn*-glycero-3-phosphocholine, 1-palmitoyl-2-stearoyl-(9,10)-dibromo-*sn*-glycero-3-phosphocholine, 1-palmitoyl-2-stearoyl-(11,12)-dibromo-*sn*-glycero-3-phosphocholine were from Avanti Polar Lipids (Alabaster, AL). 1,2-Dioleoyl-*sn*-glycero-3-phosphocholine (DOPC) was purchased from Fluka. Thiolipids, DP-mercapto-PA (*O*-(8′-mercapto-3′,6′-dioxaoctyl)-1,2-dipalmitoyl-*sn*-glycero-3-phosphatidic acid), were a gift from Horst Vogel (Lausanne, Switzerland) (29, 30). Octyl-POE was purchased from Alexis Biochemicals (San Diego, CA). All other materials were from Sigma, unless specified differently.

Preparation of EqtII and Mutants—Wild-type EqtII was isolated from the sea anemones as described earlier (31). All EqtII mutants (S114C, V8C/K69C, and tryptophan mutants W116F, W112F* (Trp-45 and Trp-149 were mutated to Phe in addition to Trp-112), and W112.116F) were prepared by site-directed mutagenesis as explained earlier (18, 32, 33). They were purified from the *Escherichia coli* cytoplasm exactly as described in (34). The fusion between the third domain of TolA (*E. coli* periplasmic protein) and EqtII was expressed in *E .coli* by the use of pTolT plasmid.[2] In this system, the third domain of the *E. coli* periplasmic TolA protein (amino acids 329–421 of SwissProt P19934) was linked to EqtII by a short flexible linker containing a thrombin cleavage site (GGGSLVPR). The fusion protein also contains six added histidines at the N terminus. Pure protein was prepared from the bacterial cytoplasm by a single purification step using Ni-nitrilotetraacetic acid agarose (Qiagen) (Fig. 3*D*) according to the manufacturer's instructions. Protein concentrations were determined spectrophotometrically by measuring the absorbance at 280 nm. Specific absorption coefficients were calculated according to the method of Perkins (35). They are 1.35 for W112F*, 1.64 for W112.116F, 1.92 for W116F, 1.51 for TolAIII-EqtII fusion, and 2.21 for the wild type and all other mutants.

Binding of Avidin to Biotinylated S114C—S114C was biotinylated as previously described (18). Excess biotin was removed on a 0.5 × 3 cm Sephadex G-15 column. Pooled active fractions were incubated with avidin (1:1, w/w) for ~1 h. The mixture was applied to a cation exchange column (SigmaChrom IEX-S, Supelco), and proteins were eluted with a gradient of salt. Biotinylated S114C bound to avidin was resolved as a single peak with a retention time different from biotinylated S114C alone and avidin. Pooled fractions were concentrated using Amicon ultrafilters (Amicon, Millipore). The protein concentration of EqtII-avidin complex was determined by BCA protein assay (Pierce).

Hemolytic Activity—Hemolytic activity was measured turbidimetrically as reported previously (36). Briefly, bovine red blood cells were extensively washed in 20 mM Tris-HCl, 130 mM NaCl, pH 7.4 (erythro-

[2] G. Anderluh, manuscript in preparation.

cyte buffer). Toxins were added to a suspension of erythrocytes with A_{700} = 0.5 at a final concentration of 3.8 nM, and the decrease in absorbance was followed for 30 min at room temperature. Time needed to achieve A_{700} = 0.250, t_{50}, was determined from the obtained traces.

Binding of Mutants to Erythrocytes—For the erythrocyte binding assays, 0.15 nmol of protein were incubated with 200 μl of bovine red blood cell suspension in erythrocyte buffer with 30 mM polyethylene glycol 3350 (A_{700} = 1.0). After 10 min of incubation on ice, erythrocytes with bound toxins were pelleted at 4 °C at 12,000 × *g* for 5 min using a benchtop centrifuge (Sigma, model 3K30). Supernatant was removed, and electrophoresis buffer was added to the pelleted erythrocytes. No additional washing steps were employed, as proteins were fully bound under these conditions and no nonspecifically bound proteins could be removed with subsequent washes (not shown). Bound proteins were resolved by SDS-PAGE on 8–25% gels using a PHAST system (Amersham Biosciences). Proteins were transferred to polyvinylidene difluoride (PVDF) membranes (Millipore) and blotted with rabbit anti-EqtII serum for 2 h. Bands were stained with goat anti-rabbit antibodies conjugated with horseradish peroxidase using 3-amino-9-ethylcarbazole/H_2O_2. Membranes were scanned using a commercial scanner, and the intensity of the bands (bound proteins) was estimated using Tina 2.0 software and expressed as a fraction of total applied protein.

Preparation of Small Unilamellar Vesicles (SUV)—Small unilamellar vesicles (SUV) were prepared as described previously (33). Briefly, chloroform was removed from the desired lipid mixture by the rotary evaporator. Vesicle buffer (140 mM NaCl, 20 mM Tris-HCl, 1 mM EDTA, pH 8.5) was added to the lipid film, and the suspension was vigorously vortex-mixed in the presence of the glass beads. The resulting multilamellar vesicles were converted to SUV by sonication (MSE 150 watts ultrasonic disintegrator) of suspension at room temperature. The SUV suspension was centrifuged at 12,000 × *g* for 15 min to remove titanium particles released from the probe. Supernatant was stored at 4 °C for up to 2 days before use.

Fluorescence Measurements—Fluorescence measurements were performed on Jasco FP-750 spectrofluorometer (Jasco Corporation, Tokyo, Japan). Unless stated otherwise, measurements were performed at 25 °C in vesicle buffer (see above). To 250 nM EqtII appropriate amounts of SUVs with or without quencher were added and tryptophan emission spectra were recorded from 310–400 nm at 125 nm/min, with excitation and emission slits set at 5 nm. Excitation wavelength was 295 nm. The intensities were corrected for the dilution factor, and the background was subtracted using appropriate blanks with SUV only. Quenching efficiency, E, for quenching of tryptophan fluorescence by bromine was calculated using the integrated area under the spectrum as in Equation 1,

$$E = 1 - (F_q/F_0) \quad \text{(Eq. 1)}$$

where F_q and F_0 are, respectively, the values in the presence and absence of the quencher. The fluorescence was integrated between 310–400 nm.

Leakage of Liposomal Contents—The leakage of encapsulated solutes was assayed as described (37). Large unilamellar vesicles (LUV) prepared as described in Caaveiro *et al.* (38) were loaded with 8-aminonaphthalene-1,3,6,-trisulfonic acid (ANTS) and *p*-xylene-*bis*-pyridiniumbromide (DPX) (both from Molecular Probes, Eugene, OR). Toxins (final 0.67 μM concentration) were added under constant stirring to the probe-loaded LUVs (at a final 0.1 mM lipid concentration, 10 mM HEPES, 200 mM NaCl, pH 7.5 at 25 °C) to reach a lipid/toxin (L/T) ratio of 150. Changes in fluorescence intensity were recorded on a PerkinElmer LS-50 spectrofluorometer (Beaconsfield, UK) with excitation and emission wavelengths set at 355 and 530 nm, respectively. An interference filter with a nominal cutoff value of 475 nm was placed in the emission light path to minimize the scattered-light contribution of the vesicles to the fluorescence signal. The percentage of leakage was calculated after all the fluorescent probe was released by the addition of the non-ionic detergent Triton X-100.

Critical Pressure Measurements—Surface pressure measurements were carried out with a MicroTrough S system from Kibron (Helsinki, Finland) at 25 °C and under constant stirring. The aqueous phase consisted of 1.1 ml of 10 mM Hepes, 200 mM NaCl, pH 7.5. The lipid, dissolved in chloroform/methanol (2:1), was gently spread over the surface and until the desired initial surface pressure was attained. The protein was injected with a Hamilton microsyringe through a hole connected to the subphase. The final protein concentration in the Langmuir trough was 1 μM. The increment in surface pressure *versus* time was recorded until a stable signal was obtained.

Preparation of Supported Planar Lipid Bilayers—A J1 chip (Biacore AB, Uppsala, Sweden) was cleaned by a freshly made piranha solution (concentrated H_2SO_4 to which 27.5% H_2O_2 was added in a ratio of 7:3) for 10 min, extensively washed with water and ethanol and finally dried in the stream of N_2. The cleaned chip was docked into the Biacore system (Biacore AB, Uppsala, Sweden), primed twice with phosphate-buffered saline and equilibrated with running buffer until a stable baseline was achieved. β-mercaptoethanol, diluted in phosphate-buffered saline to a final concentration of 1 mg/ml, was passed over the gold surface for 20 min at a flow rate of 2 μl/min. After a 1-min wash with 0.05% SDS, the thiolipids (0.4 mg/ml), diluted in 1% octyl-POE solution, were injected over the sensor surface for 5 min at a flow rate of 2 μl/min. The prepared thiolipid surface was then washed by a 1-min injection of 0.05% SDS at a flow rate of 5 μl/min. This restricted assembly resulted in 10–20% of the surface being covered with thiolipids. A suspension of SUV was then injected over the chip for 20 min at a flow rate of 2 μl/min. A spontaneously assembled lipid bilayer was formed, tethered by the previously immobilized thiolipids randomly inserted in the β-mercaptoethanol monolayer (Fig. 2*A*). Loosely bound lipids (possibly multiple bilayers) were removed by three 1-min injections of water and equilibrated in phosphate-buffered saline running buffer with a faster flow rate of 100 μl/min. A stable baseline was then achieved.

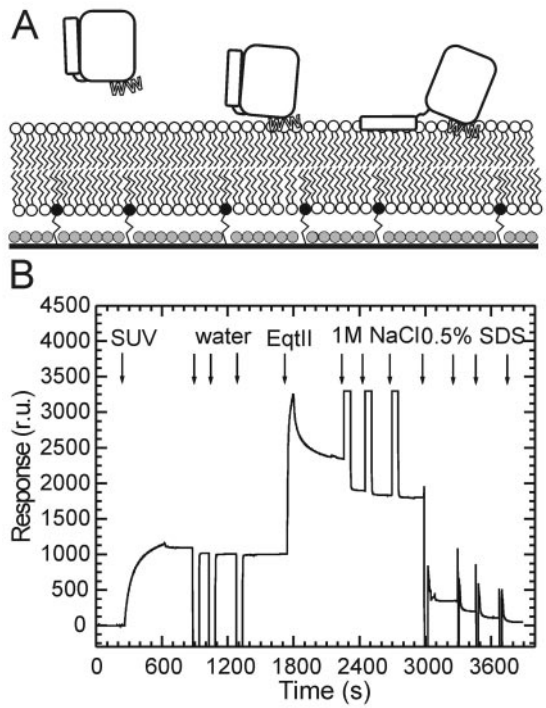

FIG. 2. **SPR binding experiment.** *A*, the overview of the SPR experiment using tethered lipid bilayers. Gold chip (*black line*) was covered with β-mercaptoethanol (*gray spheres*) and thiolipids (*black spheres* with short tether containing a thiol group, which enables the attachment to gold surface). A tethered bilayer was spontaneously formed after solution of SUV was passed over the β-mercaptoethanol-thiolipid surface. Two steps were recognized in EqtII binding. First was reversible attachment and second irreversible binding, possibly promoted by a conformational change in the region of the N-terminal α-helix. Exposed tryptophans involved in binding are designated on the model. The exact final orientation of the N-terminal helix is as yet undefined. *B*, sensorgram of binding experiment. *Arrows* designate times at which various compounds were injected over the β-mercaptoethanol-thiolipid chip surface.

Binding Measurements Using SPR—Binding of the EqtII and mutants to the membrane was measured by injecting a defined concentration of EqtII over the surface followed by a desorption step in the absence of EqtII. In some cases any remaining bound protein was then washed three times with a high salt buffer (phosphate-buffered saline with 1 M NaCl). The reported response values (Fig. 2*B*) were determined at this stage, *i.e.* the amount of stably incorporated protein. Similar binding experiments were carried out in a high salt phosphate-buffered saline running buffer, but without subsequent washes. At the end of each measurement the thiolipid chip was regenerated by few washes of 0.5% SDS, which removed the membranes along with bound proteins (Fig. 2*B*). When the baseline of the sensorgram returned to the previous

level of a mixed β-mercaptoethanol-thiolipid monolayer, a new tethered bilayer was created by the injection of SUV of the required lipid composition for the next binding experiment.

Analysis of the SPR Data—A model of EqtII binding to the lipid bilayer can be established with the scheme (Fig. 2*A*) as in Equation 2,

$$T + L \underset{k_{d1}}{\overset{k_{a1}}{\rightleftharpoons}} TL \underset{k_{d2}}{\overset{k_{a2}}{\rightleftharpoons}} TL^* \quad \text{(Eq. 2)}$$

where T corresponds to the EqtII, L corresponds to the lipid bilayer, TL is the complex of EqtII-lipid on the surface of the bilayer, and TL* is the deeply bound complex.

The initial condition and the rate equations of the binding at time $t = 0$ are: [T] = C, (the concentration of injected EqtII), [TL] = 0, [TL*] = 0. At time $t = t$, we have Equations 3–5.

$$\frac{d[L]}{dt} = -k_{a1}[T][L] + k_{d1}[TL] \quad \text{(Eq. 3)}$$

$$\frac{d[TL]}{dt} = (k_{a1}[T][L] - k_{d1}[TL]) - (k_{a2}[TL] - k_{d2}[TL^*]) \quad \text{(Eq. 4)}$$

$$\frac{d[TL^*]}{dt} = k_{a2}[TL] - k_{d2}[TL^*] \quad \text{(Eq. 5)}$$

These equations are solved for the rate constants k_a and k_d using Biacore evaluation software version 3.0. The equilibrium affinity constant K_D is calculated from Equations 6–8.

$$K_{D1} = k_{d1}/k_{a1} \quad \text{(Eq. 6)}$$

$$K_{D2} = k_{d2}/k_{a2} \quad \text{(Eq. 7)}$$

$$K_D = K_{D1}^*/K_{D2} \quad \text{(Eq. 8)}$$

RESULTS

The Aromatic Cluster Is the Principal Binding Region—According to sequence analysis (19, 38) and functional studies (18, 32, 33), the two parts of the EqtII molecule likely to interact with the membrane are the N-terminal amphiphilic helix and the tryptophan-rich cluster in the middle of the polypeptide chain. Our working hypothesis is that EqtII first attaches to the membrane via the tryptophan-rich cluster thus providing additional contacts with the membrane and secondly transfers its N-terminal helix into the lipid bilayer thus creating the walls of the transmembrane pore. Here we show the role and importance of these two parts in the pore-forming process by using different constructs to block individual stages in the pore formation (Fig. 3*A*). In particular, the binding to red blood cells and hemolytic activity were checked. These two represent the first part (binding to erythrocytes membranes) and the last part of the hemolytic process (formation of functional pores). We first tried to block the binding of EqtII to the membranes by attaching a large protein in the vicinity of the aromatic cluster. Binding should be sterically prevented and, consequently, no lysis of erythrocytes should be observed. To this end, mutant S114C was biotinylated and complexed with avidin. Ser-114, which has been shown to interact with membranes (18), is located in the middle of the tryptophan-rich cluster on the exposed loop connecting β-sheets 7 and 8. Avidin does not associate nonspecifically with the wild-type EqtII (18). The high molecular weight complex composed of S114C and avidin was formed only when the mutant was biotinylated. Membrane binding of the complex was strongly inhibited, only 6% of the total applied bound to erythrocyte membranes (Fig. 3, *C* and *F*). In comparison, 92 and 85% of native EqtII and biotinylated S114C, respectively, were bound under the experimental conditions employed. Consequently, we could not measure any hemolytic activity of the EqtII-avidin complex. Minor residual binding of the complex observed on the blot might be due to the interaction of the free N-terminal helix with the membrane. Two additional mutants were created in order to inhibit the partitioning of the N-terminal helix into the membrane and thus to block the second stage in the pore formation. The first was a fusion protein between a small globular domain of 11 kDa at the N terminus (third domain of TolA periplasmic protein from *E. coli* (39)) and EqtII at the C terminus (Fig. 3*A*). The proteins were connected by a short flexible linker, which contained a thrombin cleavage site. The extra domain prevented the translocation of the helix across the membrane, and consequently no hemolysis was observed. However, upon cleav-

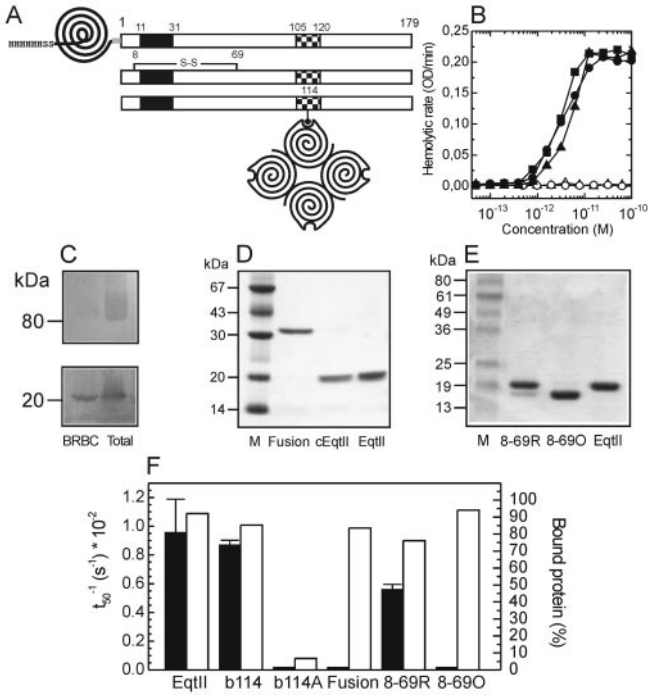

FIG. 3. **Binding and hemolytic activity of various EqtII constructs.** *A*, various constructs employed in the experiment are represented by a scheme. The N-terminal amphiphilic region (11–31) of EqtII is marked *black* and the tryptophan-rich region is *checked* (105–120). The third domain of TolA protein in the fusion protein is shown schematically (*upper panel*). The His tag at the N terminus is shown with the amino acid sequence, the flexible region between the both proteins with thrombin cleavage site (GGGSLVPR) is *gray*. The disulfide bond in the double cysteine mutant 8-69 (EqtII V8C/K69C) is denoted (*middle panel*). Biotin attached to cysteine in S114C is shown as a *black circle*. Tetrameric avidin is presented schematically (*lower panel*). *B*, hemolytic activity was measured turbidimetrically at 630 nm with a microplate reader in 20 mM Tris-HCl, 130 mM NaCl, pH 7.4. The maximum rate of hemolysis (OD/min) is reported. *Black squares*, EqtII; *open triangles*, fusion protein; *solid triangles*, released EqtII after cleavage of fusion protein; *open circles*, oxidized 8-69; *solid circles*, reduced 8-69. *C*, binding of biotinylated S114C-avidin complex (*upper panel*) or EqtII (*bottom panel*) to bovine red blood cells. Bound proteins were separated by PHAST system on 8–25% SDS-PAGE gels and blotted and stained with anti-EqtII serum and secondary antibodies conjugated with horseradish peroxidase. *D*, 12% SDS-PAGE of fusion protein. *Fusion*, fusion protein; *cEqtII*, EqtII after cleavage of fusion protein; *EqtII*, native EqtII; *M*, molecular weight marker. *E*, 10% SDS-PAGE of mutant 8-69. Mutant was reduced prior to the experiment by 10 min of incubation in 10 mM dithiothreitol. Oxidized form was prepared by preincubation with 0.5 mM phenanthroline, 0.1 mM $CuSO_4$. *8-69R*, reduced 8-69; *8-69O*, oxidized 8-69; *EqtII*, equinatoxin II; *M*, molecular weight marker. Gels were stained with Coomassie Blue. *F*, comparison of binding to bovine red blood cells and hemolytic activity of various mutant Eqts. Hemolytic activity of the constructs (*black bars*) was measured turbidimetrically on bovine red blood cells at room temperature as described (36) (n = 2–5 ± S.D.). Binding of constructs to the bovine red blood cells was analyzed by Western blots (*open bars*) using an anti-EqtII serum. The intensity of the bands was estimated after the blots (as in 3C) were scanned and percentage of bound proteins was calculated. A representative result is shown. *EqtII*, equinatoxin II; *b114*, biotinylated S114C; *b114A*, biotinylated S114C bound to avidin; *Fusion*, fusion protein of TolAIII and EqtII; *8-69R*, reduced 8-69; *8-69O*, oxidized 8-69.

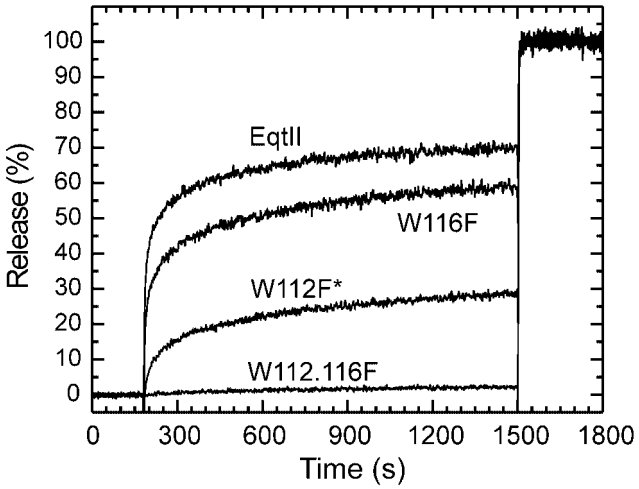

FIG. 4. **Permeabilizing activity of tryptophan mutants.** The final concentration of proteins was in all cases 0.67 μM. Proteins were added to a ANTX/DPS-loaded LUV composed of SM/PC 1/1 at a L/T ratio 150 in 10 mM HEPES, 200 mM NaCl, pH 7.5. Excitation wavelength was set to 355 nm, and fluorescence was followed at 530 nm. At the end of the experiment, t = 1500 s, the final fluorescence was obtained by adding Triton X-100 at a 0.1% (w/v) final concentration.

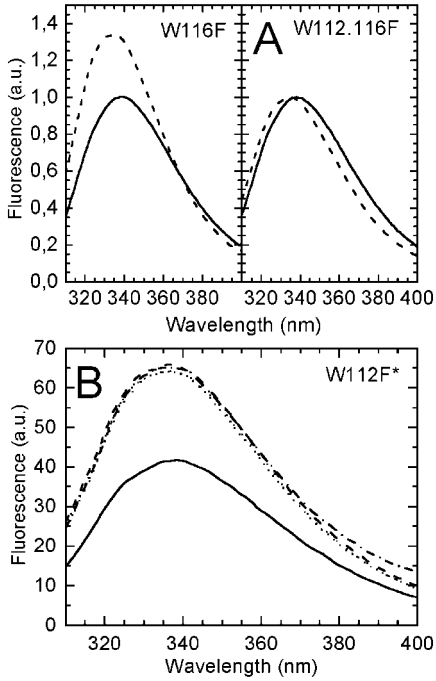

FIG. 5. **Fluorescence measurements.** The final concentration of all mutants was 250 nM in 140 mM NaCl, 20 mM Tris-HCl, 1 mM EDTA, pH 8.5. The tryptophan fluorescence was excited at 295 nm and emission scanned between 310 and 400 nm at 25 °C. *A*, fluorescence in solution (*solid line*) or in the presence of SM/DPPC SUV (*dashed line*). *B*, fluorescence of W112F* in solution (*solid line*), in the presence of SM/DPPC SUV (*dashed line*), or SM/PC Br SUV with bromine at positions 6–7 (*dotted line*), 9–10 (*dash-dotted line*), or 11–12 (*short dashed line*). The L/T ratio was 200 in all cases.

age a properly folded and fully active EqtII was released (Fig. 3, *B* and *D*). The second was the double cysteine mutant V8C/K69C (designated throughout the paper as 8-69), in which the N-terminal helix was fixed to the body of the molecule by a disulfide bridge between the introduced cysteines (Figs. 1*A* and 3*A*). This mutant has similar structural properties to EqtII as judged from fluorescence and far-UV CD spectra (data not shown). Furthermore, there were no major structural differences observed between the oxidized and reduced form. Introduced cysteines enabled formation of an intramolecular disulfide bond. No higher-order aggregates were observed on the SDS-PAGE (Fig. 3*E*), hence the oxidized form was a homogeneous monomer. In the oxidized form, the helix should remain attached to the body of the molecule after initial binding and should not translocate into the membrane. As expected, 8-69 was not hemolytically active, unless first reduced with dithiothreitol (Fig. 3*B*). Both of these constructs bound normally to the lipid-water interface, because the tryptophan cluster was not affected (Fig. 3*F*). Thus, in these cases the helix was unable to translocate fully into the lipid bilayer, either due to steric hindrances (in the case of the fusion protein) or due to lack of mobility (double cysteine mutant). These results clearly demonstrate that the tryptophan-rich region is the principal binding site for the EqtII and that the free N-terminal helix is required in subsequent steps of the pore-forming process.

Tryptophan Mutants from the Aromatic Cluster—As tryptophans are mainly responsible for the anchoring of proteins within water-lipid interface of the membranes (22, 23), the effect of tryptophans 112 and 116 (within the aromatic cluster) on the permeabilizing activity and binding was further analyzed. Three tryptophan mutants (W116F, W112F*, and W112.116F) were prepared by mutating tryptophans to phenylalanines leaving either just one (Trp-112 or Trp-116), or no, tryptophans within the aromatic cluster. Mutant W112F* was included in the study since it had been already well characterized, both structurally and functionally with structural properties indistinguishable from that of EqtII (33). The asterisk denotes two additional tryptophans, 45 and 149, which were mutated in this mutant to phenylalanines. They were shown not to be important for maintaining the three-dimensional structure of W112F*, neither do they interact with the lipid membrane (33). The mutations in W116F and W112.116F did not structurally alter the mutants, as evidenced by their similar melting temperatures relative to EqtII in far-UV CD measurements or ANS binding assay (data not shown). All the mutants were checked for release of fluorescent markers from LUV (Fig. 4). In the ANTS/DPX system the final release from SM/PC 1/1 LUV at a L/T ratio of 150 was 69.7 ± 0.3, 57.3 ± 2.1, 27.2 ± 1.7 and 2.3 ± 0.2 (n = 2 ± S.D.) for the EqtII, W116F, W112F*, and W112.116F, respectively. All the mutants were thus consistently less active than the wild type. These data indicate that tryptophans from the aromatic cluster are needed for the permeabilizing activity. Changes of tryptophan fluorescence upon binding, insertion into lipid monolayers and binding to supported lipid bilayers were checked next, in order to see whether the decrease in permeabilizing activity is the result of reduced binding.

Fluorescence Measurements—Binding of EqtII to the lipid bilayer resulted in a blue-shift of the intrinsic fluorescence reflecting the transfer of exposed tryptophan residues to the more hydrophobic lipid phase (14, 33). We have shown in a previous study that EqtII and W112F* exhibited similar blue shifts and fluorescence increases, indicating transfer of Trp-116 in the lipid phase (33). On the contrary Trp-45 and Trp-149 were found not to associate significantly with the membrane. Here we further show that Trp-112 is also inserted into the lipid bilayer (Fig. 5*A*). Mutant W116F exhibited a blue-shift of the emission maximum from 339 to 334 nm that was accompanied by an increase in tryptophan fluorescence. W112.116F showed little change on lipid addition, which is in accordance with the lack of insertion of the remaining tryptophans into the membranes (Fig. 5*A*, *right panel*) (33). The small blue shift might be attributed to a decrease of dielectric constant near the surface of the membrane, which could influence the fluorescence of other tryptophans close to the aromatic region (*i.e.* 117

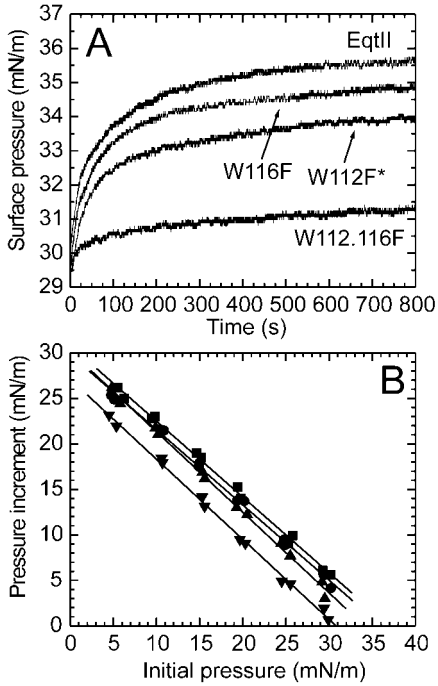

FIG. 6. **Insertion into monolayers.** *A*, time traces of insertion at π_0 = 30 mN/m at room temperature and with constant stirring. The concentration of proteins was 1 μM in 10 mM Hepes, 200 mM NaCl, pH 7.5. Monolayers were composed of SM/PC 1/1. *B*, effect of initial surface pressure on the insertion of proteins in the monolayers. Experimental data from two independent experiments were fitted to straight lines whose intercepts with the abscissa axis represent the critical pressure (π_c). Other experimental conditions are as in *A*. *Squares*, EqtII; *circles*, W116F; *triangles*, W112F*; *inverted triangles*, W112.116F.

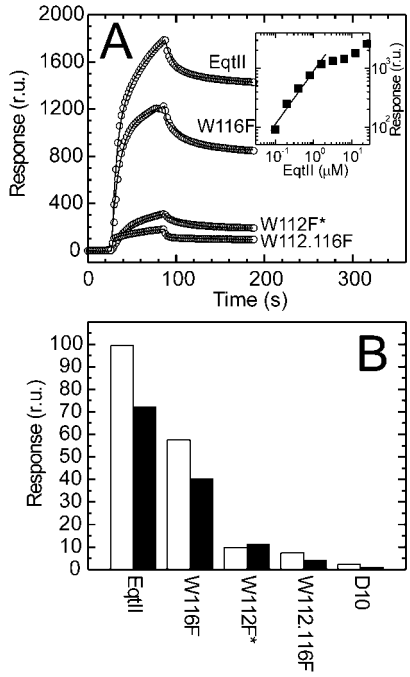

FIG. 7. **Binding of EqtII and mutants measured by SPR.** *A*, binding of EqtII and tryptophan mutants to the tethered lipid bilayer composed of DOPC/SM 1/1. The concentration of proteins in the running high-salt buffer (0.1 M phosphate-buffered saline, 1 M NaCl, pH 7.0) was 1 μM. The experimental data (*circles*) were fitted to a two step binding model (*curve*) presented under "Experimental Procedures." The *inset* shows the response at different EqtII concentrations. *B*, binding of EqtII and different mutants to DOPC/SM 1:1 membranes in low (*open bars*) or high salt (*black bars*). The concentration of proteins was always 1 μM. D10 is a control protein, which has similar biochemical properties as EqtII (M_r = 18.6, pI = 9.4 for D10 and M_r = 19.8, pI = 10.5 for EqtII) but no known membrane binding affinity. It was used as a control for nonspecific binding.

or 149). Brominated lipids were used in order to measure the depth of the insertion in the lipid bilayer. Bromine is a short range quencher, having an R_0, the distance at which 50% of quenching occurred, of 0.925 nm (40, 41). This means that tryptophans need to come in close proximity to the bromine in order to be quenched. SUV composed of an equimolar mixture of SM and DPPC or brominated PC were used. The L/T ratio was kept at 200. Under these conditions the binding of W112F* to the SUV was almost complete as measured by residual hemolytic activity. This was confirmed also by a similar blue-shift in brominated vesicles when compared with vesicles without quencher (Fig. 5*B*), indicating that Trp-116 is fully transferred to the lipid bilayer. However, none of the brominated lipids was able to quench the fluorescence of W112F*. The efficiency of quenching, E, was 3.0 ± 0.04, −1.1 ± 0.05, and 3.2 ± 0.02 (n = 4 ± S.D.) for SUV of PC containing bromine at positions 6–7, 9–10, and 11–12 respectively. These results indicate that Trp-116 does not penetrate even to the vicinity of the shallowest quencher with bromine at positions 6–7. Similar results were obtained with the wild-type EqtII,[3] indicating that even Trp-112, as the most exposed, is not inserting deeply into the acyl chain part of the lipid bilayer.

Insertion into the Lipid Monolayers—Insertion of EqtII and tryptophan mutants was monitored on monolayers composed of an equimolar mixture of PC and SM (Fig. 6). The insertion of the proteins into the monolayer increased the surface pressure, $\Delta\pi$, from the chosen initial pressure level, π_0. The insertion differed markedly among the mutants; at 30 mN/m all mutants inserted less and more slowly than EqtII. The worst was W112.116F, which barely inserted (Fig. 6*A*). $\Delta\pi$ was measured next at different π_0 values (Fig. 6*B*). $\Delta\pi$ decreased with increasing π_0 for all proteins, because tighter lipid packing prevented insertion. It is possible to determine the critical pressure π_c, *i.e.* the pressure at which no protein is inserted into the lipid bilayer, by extrapolating the data from Fig. 6*B* to the point at which $\Delta\pi$ = 0. Removal of tryptophans resulted in a decrease in π_c. Values determined were 37.0, 36.1, 34.1, and 30.8 mN m^{-1} (from two independent experiments) for EqtII, W116F, W112F*, and W112.116F, respectively. The slope of the fitted curves was very similar in all cases, suggesting that the final inserted state of the different mutants is the same.

Binding to the Supported Planar Bilayers—Membrane binding of tryptophan mutants was also checked by SPR, an increasingly popular technique for measuring protein-membrane interactions. Usually immobilized lipid vesicles or bilayers formed on a hydrophobic surface are used (42–45). We have chosen a membrane bilayer tethered to the gold chip by thiolipids (Fig. 2*A*), which provides a well defined model membrane in which both upper and lower layers are fluid (29). To ensure that the tethered bilayer is comparable to other model bilayer systems we first showed that EqtII binds specifically only to the tethered bilayer (Fig. 7*A*). There was no binding to the chip alone or the incomplete hybrid monolayer of thiolipids and β-mercaptoethanol. EqtII binds to tethered membranes in a dose-dependant fashion (Fig. 7*A*, *inset*). The experimental points from the linear part of a double reciprocal graph were linearly fitted to yield a slope (k) of 0.90 ± 0.09 (n = 5, r = 0.98; p = 0.02), thus suggesting that binding at low EqtII concentrations, as a first step in pore formation, is non-cooperative. The binding is almost irreversible, and it was not possible to

[3] I. Gutiérrez-Aguirre and J. M. González-Mañas, unpublished observations.

TABLE I

Rate and affinity constants for binding of EqtII and mutants to tethered bilayers

The rate constants were determined from sensorgrams recorded for the binding of wild-type and mutants to tethered lipid bilayers composed of DOPC/SM 1/1 according to the binding model described under "Experimental Procedures." The representative result is shown. The standard error of the fit is reported in parentheses. Affinity constants, K_D, were calculated using Equation 6.

Protein	k_{a1}	k_{d1}	k_{a2}	k_{d2}	K_{D1}	K_{D2}	K_D
	$M^{-1}\,s^{-1} \times 10^5$	$s^{-1} \times 10^{-2}$	$s^{-1} \times 10^{-2}$	$s^{-1} \times 10^{-4}$	$M \times 10^{-7}$	$\times 10^{-2}$	$M \times 10^{-8}$
EqtII	0.9 (0.011)	0.8 (0.05)	0.9 (0.014)	7.5 (0.73)	0.9	8.3	0.75
EqtII 1M NaCl	0.8 (0.007)	9 (0.02)	3.1 (0.007)	4.4 (0.05)	11.3	1.4	1.6
W116F	0.9 (0.011)	3.9 (0.064)	2.2 (0.02)	4.7 (0.1)	4.3	2.1	0.9
W112F*	1.0 (0.014)	3.9 (0.036)	1.1 (0.013)	15.5 (0.26)	3.9	14.1	5.5
W112.116F	1.1 (0.017)	13.3 (0.19)	2.2 (0.03)	13.9 (0.3)	12.1	6.3	7.6
8–69 reduced	1.0 (0.008)	2.8 (0.06)	2.3 (0.033)	10.4 (0.1)	2.8	4.5	1.3
8–69 oxidized	1.4 (0.017)	3.3 (0.053)	1.9 (0.019)	20.6 (0.21)	2.4	10.8	2.6

remove the EqtII from the supported bilayer by washing with water, 2 M salt or 10 mM glycine, pH 2. The absolute binding level was higher in low salt buffer (0.1 M phosphate-buffered saline, pH 7.0) than in the presence of 1 M salt, where it was reduced by ~30%. A control protein D10 (a fusion of *E. coli* TolA third domain (TolAIII) and colicin NT domain (colN)),[4] which has similar biochemical properties (M_r = 18.6, pI = 9.4 for TolAIII-colN fusion and M_r = 19.8, pI = 10.5 for EqtII) but no known membrane binding affinity, was used as a control for unspecific binding. D10 showed negligible binding in this system (Fig. 7*B*). Mutants were checked for binding on DOPC/SM 1/1 membranes in the presence of low or high salt (Fig. 7). As with EqtII, the binding was always lower in the presence of the high salt, with the exception of W112F*, which binds similarly in both conditions. All mutants tested bound less strongly than EqtII. Trp-112 was found to be the most critical since the mutation of this residue almost completely prevented binding of W112F* and W112.116F (Fig. 7).

It was not possible to fit the SPR data reliably to a 1:1 Langmuir binding model. We, therefore, used a two state kinetic model, which is the next simplest and can also be correlated to the hypothetical insertion sequence proposed in Equation 2 and Fig. 2*A* (see "Experimental Procedures"): adsorption onto the membrane surface and then insertion, possibly promoted by a conformational change. The conformational change might expose additional regions, *i.e.* the N-terminal α-helix, which further interacts with the membrane and would lead to a stable insertion of the EqtII into the bilayer. Detailed binding parameters for EqtII and mutants are reported in Table I.

Insertion and Binding of the Double Cysteine Mutant 8-69—In order to discriminate between the two steps in the proposed model, the membrane binding of the double cysteine mutant 8-69 was checked with monolayers and SPR in both reduced and oxidized forms (Fig. 8). The reduced form showed wild-type insertion and binding, whereas the oxidized form showed qualitatively and quantitatively different traces, both on monolayers and bilayers (Fig. 8). At each π_0 it inserts less into monolayers than EqtII or the reduced form (Fig. 8*A*). This leads to a distinctly different slope of the regression lines in critical pressure plot (Fig. 8*A, inset*). The slopes were −0.86 for the reduced form and −0.62 for the oxidized form. However, the π_c is similar for both, 36.0 and 36.4 mN/m for the reduced and oxidized forms, respectively. The smaller area occupied by the mutant due to helix restriction can explain the reduced insertion observed at each initial pressure since only the aromatic cluster is positioned within the monolayer. Additional insertion was observed when 10 mM dithiothreitol was added to the oxidized mutant after it was stably inserted in the monolayer (Fig. 8*A*). In the SPR experiment the reduced form bound similarly to EqtII, while the oxidized form bound less with a distinctly different dissociation phase (Fig. 8*B*). The obtained parameters from the fit are presented in Table I and indicate that the disulfide bridge predominately inhibits the second phase of binding.

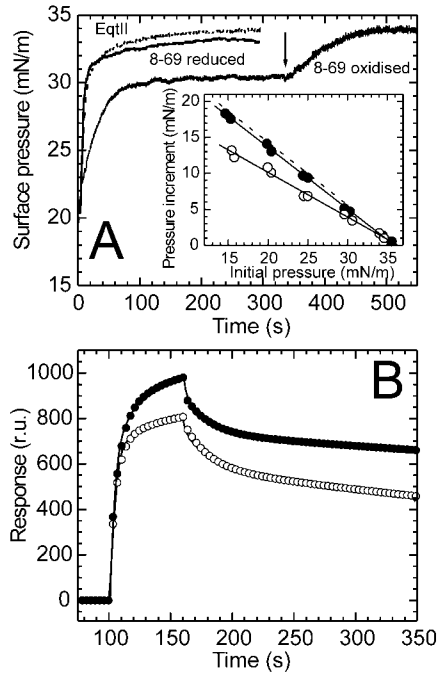

FIG. 8. **Insertion and binding of double cysteine mutant 8-69.** *A*, insertion of 8-69 in reduced and in oxidized form. Mutant was reduced prior to the experiment by 10 min incubation in 10 mM dithiothreitol. Oxidized form was prepared by preincubation with 0.5 mM phenanthroline, 0.1 mM $CuSO_4$. The data obtained for EqtII from Fig. 6 are shown for comparison (*dashed line*). 10 mM final dithiothreitol was added at the time indicated by an *arrow*. Other experimental conditions are as in Fig. 6. *Inset*, critical pressure plot for 8-69 in oxidized and reduced form. The data obtained for EqtII from Fig. 6 are shown for comparison (*dashed line*). *B*, sensorgrams of reduced (*black circles*) and oxidized (*white circles*) forms of 8-69. Mutant was treated prior experiment as in *A*. The fits of the experimental data are shown with *black lines*. Other experimental conditions are as in Fig. 7.

DISCUSSION

We have been studying the binding of EqtII and various mutants to model membranes by using monolayers and SPR. We show for the first time that the actinoporin binding to lipid membranes is a two step process (Fig. 2*A*). The data are consistent with two modes of interaction: a weak binding step followed by a conformational change and irreversible insertion.

The Role of Electrostatic Interactions and Aromatic Residues—The binding of proteins to lipid membranes results from a mixture of electrostatic and hydrophobic interactions (46). As deduced from Fig. 7*B*, the effect of mutating the side chains of

[4] G. Anderluh and J. H. Lakey, unpublished data.

crucial tryptophans in the aromatic cluster was much more pronounced than that of high concentrations of salt. The binding was reduced by ~30% when high salt buffer was used (*i.e.* the binding of EqtII in the absence or presence of the salt), but it was decreased by more than 90% when tryptophans 112 and 116 were mutated (*i.e.* the binding of EqtII and W112.116F in low salt buffer). This indicates that interactions involving tryptophans are more important than electrostatic ones. Nevertheless, from SPR kinetic data, high salt decreases the residence time of EqtII on the membrane and affects both k_{d1} and k_{a2} showing that electrostatic interactions play a role in both stages of the interaction. In a recent study Valcarcel *et al.* (47) showed that sticholysin, a homologue of EqtII from *Stichodactyla helianthus*, loses its permeabilizing activity on zwitterionic membranes composed of PC/SM 1/1 when the salt concentration is increased. The authors suggested that the decreased permeabilizing activity might be due to the absence of conformational change needed for binding, which is accounted for by strengthening hydrophobic forces within the protein in high salt concentration. We indeed observed an 11-fold increase in k_{d1} when the high salt buffer was used, inhibiting the second conformationally coupled step which in turn decreases the membrane residence time of adsorbed toxin resulting in an increased K_{D1}.

The mutation of tryptophans to phenylalanines in the aromatic cluster mostly changes the residence time of the EqtII on the membrane, *i.e.* the mutations destabilize the protein-membrane complex. While the changes in association constants are not so pronounced, the changes in dissociation constants are substantial. The largest effect was observed with W112.116F. The dissociation rate for this mutant was much faster than for any other mutant. The 17-fold increase in k_{d1} resulted in a K_{D1} 14-fold higher. This clearly indicates the role of tryptophans 112 and 116 in stabilizing the adsorbed EqtII on the membrane during the initial contact. After the initial binding, the dissociation constant is more or less the same (K_{D2} varies less than K_{D1}). Here the tryptophan's role is diminished, and other regions might be responsible for deeper insertion, *e.g.* the N-terminal helix.

The Role of the N-terminal Helix—The N-terminal helix was proposed to participate in the final phases of the pore formation (17–19). Here we show that it can also participate in the membrane binding of EqtII. It has a minor role, as mutants with an obstructed helix can still show significant binding to membranes (Figs. 3 and 8). We were able to distinguish two steps in the binding mechanism by the use of the double cysteine mutant. The N-terminal helix participates in the binding only after EqtII attaches to membranes with aromatic cluster. This is nicely demonstrated by the use of the double cysteine mutant with monolayer technique. When dithiothreitol was added to the oxidized mutant fully inserted to monolayer an additional increase was observed (Fig. 8*A*). The increase of 25–30% correlates well with the difference in slopes, 27.9%, of oxidized and reduced forms in the critical pressure plot (Fig. 8*A*, *inset*). The difference between the two slopes can be an estimation of the change in area occupied by each protein, and this change can be, therefore, attributed solely to the N-terminal helix.

Two steps were also resolved by the SPR. The attachment of the N-terminal helix to the body of the molecule by the disulfide bridge mainly changes k_{d2} as viewed from kinetic data. It is doubled in the oxidized form in comparison to the reduced one (Table I), while other parameters do not vary substantially. This increase in the k_{d2} supports the hypothesis that the second stage is a more deeply associated form anchored by the N-terminal helix. Nevertheless, since the second stage is not entirely abolished by oxidation, it must be assumed that the helix is one of the components involved in this conformational change.

Comparison with other Proteins—A number of small globular domains have been reported to bind to membrane surfaces by the combination of electrostatic and hydrophobic interactions (1, 2, 23, 48, 49). The common theme for all of them is small size, compactness, high content of β-sheet structure and usually exposed aromatic amino acids. One such example are domains of bacterial PFT. Results provided here for binding of EqtII are reminiscent of the binding of CDC. Not only is there a structural similarity (20), but actinoporins and CDC share also functional similarity. In both cases shallow binding mediated by exposed aromatic amino acids is promoted by a relatively small, β-sandwich domain; however, later steps in pore formation are completed by other different parts of the molecule. In CDC toxins a pore is formed by a huge transmembrane β-barrel composed from other domains (50, 51), while in actinoporins further binding and pore-formation is provided by the amphiphilic helix, a structural motif characteristic of antimicrobial peptides (8, 10). Apparently, convergent evolution provided toxins in evolutionary distant organisms, bacteria and sea anemones, with a structurally and functionally similar membrane binding domain. It should be noted however that, although CDC are specific for cholesterol, the exact mechanism of cholesterol recognition at the molecular level is not yet understood (25). Interestingly, it was shown recently, that EqtII and sticholysin show higher permeabilizing activity if cholesterol is present in the membranes (38, 52), which allude to another similarity between both types of toxins.

In conclusion, we provide structural and kinetic evidence that EqtII binds to membrane in a two stage process, each promoted by separate regions: the tryptophan-rich cluster and the N-terminal helix. By the use of monolayer and supported bilayer SPR techniques we are able, for the first time, to separately analyze the two stages and show that the initial binding site is the aromatic cluster. If this is sterically shielded, or has key residues mutated, the binding to the membranes was largely abolished. The N-terminal helix is involved in the second stage of membrane insertion because both obstruction of the N-terminal helix or its immobilization with the disulfide bond did not inhibit the initial binding interaction. Similar domains are found in other peripheral membrane proteins, indicating that this is a widely occurring mechanism for targeting to the membranes.

Acknowledgments—We thank Dr. Gianfranco Menestrina and Prof. Richard Virden for critical reading of the manuscript, Dr. Gregor Gunčar for the help during the preparation of Fig. 1*B*, and Irena Pavešić for technical assistance. The thiolipid was a kind gift from Horst Vogel.

REFERENCES

1. Hurley, J. H., and Misra, S. (2000) *Annu. Rev. Biophys. Biomol. Struct.* **29,** 49–79
2. Cho, W. (2001) *J. Biol. Chem.* **276,** 32407–32410
3. Lemmon, M. A., Ferguson, K. M., and Schlessinger, J. (1996) *Cell* **85,** 621–624
4. Driscoll, P. C., and Vuidepot, A. L. (1999) *Curr. Biol.* **9,** R857-R860
5. Ferguson, K. M., Lemmon, M. A., Schlessinger, J., and Sigler, P. B. (1995) *Cell* **83,** 1037–1046
6. Kim, K. P., Han, S. K., Hong, M., and Cho, W. (2000) *Biochem. J.* **348,** 643–647
7. van der Goot, G. (2001) *Pore-Forming Toxins. Current Topics in Microbiology and Immunology*, Springer, Berlin, Germany
8. Zasloff, M. (2002) *Nature* **415,** 389–395
9. Parker, M. W. (1996) *Protein Toxin Structure*, Springer-Verlag, Heidelberg, Germany
10. Anderluh, G., and Maček, P. (2002) *Toxicon* **40,** 111–124
11. Kem, W. R. (1988) in *The Biology of the Nematocyst* (Hessinger, D. A., Lenhoff, H. M., ed), pp. 375–405, Academic Press, San Diego
12. Belmonte, G., Pederzolli, C., Maček, P., and Menestrina, G. (1993) *J. Membr. Biol.* **131,** 11–22
13. Zorec, R., Tester, M., Maček, P., and Mason, W. T. (1990) *J. Membr. Biol.* **118,** 243–249
14. Maček, P., Zecchini, M., Pederzolli, C., Dalla Serra, M., and Menestrina, G. (1995) *Eur. J. Biochem.* **234,** 329–335
15. Maček, P., Belmonte, G., Pederzolli, C., and Menestrina, G. (1994) *Toxicology*

87, 205–227
16. Tejuca, M., Dalla Serra, M., Ferreras, M., Lanio, M. E., and Menestrina, G. (1996) *Biochemistry* **35,** 14947–14957
17. Anderluh, G., Pungerčar, J., Križaj, I., Štrukelj, B., Gubenšek, F., and Maček, P. (1997) *Protein Eng.* **10,** 751–755
18. Anderluh, G., Barlič, A., Podlesek, Z., Maček, P., Pungerčar, J., Gubenšek, F., Zecchini, M. L., Dalla Serra, M., and Menestrina, G. (1999) *Eur. J. Biochem.* **263,** 128–136
19. Belmonte, G., Menestrina, G., Pederzolli, C., Križaj, I., Gubenšek, F., Turk, T., and Maček, P. (1994) *Biochim. Biophys. Acta-Biomembr.* **1192,** 197–204
20. Athanasiadis, A., Anderluh, G., Maček, P., and Turk, D. (2001) *Structure* **9,** 341–346
21. Hinds, M. G., Zhang, W., Anderluh, G., Hansen, P. E., and Norton, R. S. (2002) *J. Mol. Biol.* **315,** 1219–1229
22. Killian, J. A., and von Heijne, G. (2000) *Trends Biochem. Sci.* **25,** 429–434
23. Kennedy, M. W., and Beauchamp, J. (2000) *Cell. Mol. Life Sci.* **57,** 1379–1387
24. Wimley, W. C., and White, S. H. (1996) *Nat. Struct. Biol.* **3,** 842–848
25. Tweten, R. K., Parker, M. W., and Johnson, A. E. (2001) *Curr. Top. Microbiol. Immunol.* **257,** 15–33
26. Rossjohn, J., Feil, S. C., McKinstry, W. J., Tweten, R. K., and Parker, M. W. (1997) *Cell* **89,** 685–692
27. Heuck, A. P., Hotze, E. M., Tweten, R. K., and Johnson, A. E. (2000) *Mol. Cell.* **6,** 1233–1242
28. Sekino-Suzuki, N., Nakamura, M., Mitsui, K., and Ohno-Iwashita, Y. (1996) *Eur. J. Biochem.* **241,** 941–947
29. Lang, H., Duschl, C., and Vogel, H. (1994) *Langmuir* **10,** 197–210
30. Terrettaz, S., Ulrich, W.-P., Vogel, H., Hong, Q., Dover, L. G., and Lakey, J. H. (2002) *Protein Sci.* **11,** 1917–1925
31. Maček, P., and Lebez, D. (1988) *Toxicon* **26,** 441–451
32. Anderluh, G., Barlič, A., Križaj, I., Menestrina, G., Gubenšek, F., and Maček, P. (1998) *Biochem. Biophys. Res. Commun.* **242,** 187–190
33. Malovrh, P., Barlič, A., Podlesek, Z., Maček, P., Menestrina, G., and Anderluh, G. (2000) *Biochem. J.* **346,** 223–232
34. Anderluh, G., Pungerčar, J., Štrukelj, B., Maček, P., and Gubenšek, F. (1996) *Biochem. Biophys. Res. Commun.* **220,** 437–442
35. Perkins, S. J. (1986) *Eur. J. Biochem.* **157,** 169–180
36. Maček, P., and Lebez, D. (1981) *Toxicon* **19,** 233–240
37. Ellens, H., Bentz, J., and Szoka, F. C. (1985) *Biochemistry* **24,** 3099–3106
38. Caaveiro, J. M. M., Echabe, I., Gutiérrez-Aguirre, I., Nieva, J. L., Arrondo, J. L. R., and González-Mañas, J. M. (2001) *Biophys. J.* **80,** 1343–1353
39. Lubkowski, J., Hennecke, F., Pluckthun, A., and Wlodawer, A. (1999) *Struct. Fold. Des.* **7,** 711–722
40. González-Mañas, J. M., Lakey, J. H., and Pattus, F. (1992) *Biochemistry* **31,** 7294–7300
41. East, J. M., and Lee, A. G. (1982) *Biochemistry* **21,** 4144–4151
42. Cho, W. W., Bittova, L., and Stahelin, R. V. (2001) *Anal. Biochem.* **296,** 153–161
43. Kuziemko, G. M., Stroh, M., and Stevens, R. C. (1996) *Biochemistry* **35,** 6375–6384
44. MacKenzie, C. R., Hirama, T., Lee, K. K., Altman, E., and Young, N. M. (1997) *J. Biol. Chem.* **272,** 5533–5538
45. Stahelin, R. V., and Cho, W. H. (2001) *Biochemistry* **40,** 4672–4678
46. Ladokhin, A. S., and White, S. H. (2001) *J. Mol. Biol.* **309,** 543–552
47. Valcarcel, C. A., Dalla Serra, M., Potrich, C., Bernhart, I., Tejuca, M., Martinez, D., Pazos, F., Lanio, M. E., and Menestrina, G. (2001) *Biophys. J.* **80,** 2761–2774
48. Pratt, K. P., Shen, B. W., Takeshima, K., Davie, E. W., Fujikawa, K., and Stoddard, B. L. (1999) *Nature* **402,** 439–442
49. Macedo-Ribeiro, S., Bode, W., Huber, R., Quinn-Allen, M. A., Kim, S. W., Ortel, T. L., Bourenkov, G. P., Bartunik, H. D., Stubbs, M. T., Kane, W. H., and Fuentes-Prior, P. (1999) *Nature* **402,** 434–439
50. Shepard, L. A., Heuck, A. P., Hamman, B. D., Rossjohn, J., Parker, M. W., Ryan, K. R., Johnson, A. E., and Tweten, R. K. (1998) *Biochemistry* **37,** 14563–14574
51. Shatursky, O., Heuck, A. P., Shepard, L. A., Rossjohn, J., Parker, M. W., Johnson, A. E., and Tweten, R. K. (1999) *Cell* **99,** 293–299
52. De los Rios, V., Mancheno, J. M., Lanio, M. E., Onaderra, M., and Gavilanes, J. G. (1998) *Eur. J. Biochem.* **252,** 284–289
53. Holm, L., and Sander, C. (1993) *J. Mol. Biol.* **233,** 123–138
54. Nicholls, A., Sharp, K. A., and Honig, B. (1991) *Proteins* **11,** 281–296